Nicotinamide Riboside Alleviates Corneal and Somatic Hypersensitivity Induced by Paclitaxel in Male Rats

Marta V. Hamity,[1] Sandra J. Kolker,[1] Deborah M. Hegarty,[2] Christopher Blum,[1] Lucy Langmack,[1] Sue A. Aicher,[2] and Donna L. Hammond[1,3]

[1]Department of Anesthesia, University of Iowa, Iowa City, Iowa, United States
[2]Department of Chemical Physiology and Biochemistry, Oregon Health & Science University, Portland, Oregon, United States
[3]Department of Neuroscience and Pharmacology, University of Iowa, Iowa City, Iowa, United States

Correspondence: Donna L. Hammond, Department of Anesthesia, 25 S Grand Avenue 3000 ML, Iowa City, IA 52242, USA; donna-hammond@uiowa.edu.

Received: July 22, 2021
Accepted: December 28, 2021
Published: January 27, 2022

Citation: Hamity MV, Kolker SJ, Hegarty DM, et al. Nicotinamide riboside alleviates corneal and somatic hypersensitivity induced by paclitaxel in male rats. *Invest Ophthalmol Vis Sci.* 2022;63(1):38. https://doi.org/10.1167/iovs.63.1.38

Purpose. Patients receiving chemotherapy may experience ocular discomfort and dry eye–like symptoms; the latter may be neuropathic in nature. This study assessed corneal and somatic hypersensitivity in male rats treated with paclitaxel and whether it was relieved by nicotinamide riboside (NR).

Methods. Corneal sensitivity to tactile and chemical stimulation, basal tear production, and sensitivity of the hindpaw to tactile and cool stimuli were assessed before and after paclitaxel in the absence and presence of sustained treatment with 500 mg/kg per os NR. Corneal nerve density and hindpaw intraepidermal nerve fiber (IENF) density were also examined.

Results. Paclitaxel-treated rats developed corneal hypersensitivity to tactile stimuli, enhanced sensitivity to capsaicin but not hyperosmolar saline, and increased basal tear production. Corneal nerve density visualized with anti–β-tubulin or calcitonin gene-related peptide (CGRP) was unaffected. Paclitaxel induced tactile and cool hypersensitivity of the hindpaw and a loss of nonpeptidergic hindpaw IENFs visualized with anti-protein gene product (PGP) 9.5 and CGRP. NR reversed tactile hypersensitivity of the cornea without suppressing tear production or chemosensitivity; it did not alter corneal afferent density. NR also reversed tactile and cool hypersensitivity of the hindpaw without reversing the loss of hindpaw IENFs.

Conclusions. These findings suggest that paclitaxel may be a good translational model for chemotherapy-induced ocular discomfort and that NR may be useful for its relief. The ability of NR to relieve somatic tactile hypersensitivity independent of changes in sensory nerve innervation suggests that reversal of terminal arbor degeneration is not critical to the actions of NR.

Keywords: chemotherapy-induced peripheral neuropathy, corneal hypersensitivity, ocular discomfort, pain, paclitaxel

Dry eye syndrome (DES) is a significant age-related health care problem that affects up to 30% of the population.[1] Painful DES shares many features of neuropathic pain and has been proposed to be a type of neuropathic pain.[2,3] Tear dysfunction may be an initiating event in painful DES in that sustained disruption of tear homeostasis may lead to repeated or sustained injury of the afferent nerves that innervate the cornea, as well as subsequent neurogenic inflammation and release of inflammatory agents in the cornea. In addition to responding to chemical, mechanical, or cooling stimuli, corneal afferents play an important role in regulating tear production.[4–6] Thus, a feed-forward cycle of maladaptive changes may be initiated. Patients undergoing paclitaxel treatment report significant ocular discomfort and symptoms akin to DES that can persist after completion of chemotherapy, particularly if they also have peripheral neuropathy.[7–9] Paclitaxel is a microtubule-stabilizing agent and interferes with mitosis. The cornea may be vulnerable to paclitaxel because it contains rapidly proliferating cells (limbal epithelial stem cells)[10] and neural crest–derived progenitor cells.[11,12] In addition, nerve terminal arborizations in the cornea epithelium remodel continuously.[5] Patients with ocular discomfort and peripheral neuropathy also exhibited a significant decrease in the length and density of nerves in the subbasal nerve plexus,[13] analogous to the "dying back" of intraepidermal nerve fibers (IENFs) documented in the skin after paclitaxel chemotherapy.[13,14]

A number of preclinical studies suggest that neuropathic pain can be relieved by nicotinamide riboside (NR), a member of the vitamin B3 family and precursor of NAD^+.[15,16] For example, NR can alleviate heat hypoalgesia, normalize deficits in nerve conduction velocity, and protect against the loss of corneal and IENFs in prediabetic and type 2 diabetic mice.[17] NR also protects mice against noise-induced hearing loss and damage to neurites of spiral

ganglia neurons.[18] In female rats, daily oral dosing with NR can prevent or reverse hypersensitivity to tactile and cooling stimuli induced by paclitaxel, a chemotherapeutic agent.[19,20] Preventive treatment with NR also obtunds the loss of IENFs in the hindpaw induced by paclitaxel.[20] These observations, particularly the possible link between DES and injury to corneal afferents, led us to ask (1) whether paclitaxel induced corneal hypersensitivity to tactile and chemical stimuli in the rat and (2) whether it could be prevented by NR.

Methods and Materials

Animals

These studies were approved by the University of Iowa Animal Care and Use Committee and conducted in accordance with the ARVO Statement for the Use of Animals in Ophthalmic and Vision Research. Male Sprague-Dawley rats (Charles River Laboratory; 150–175 g) were housed on a 12:12-hour light/dark cycle with ab libitum access to food and water. Rats received three intravenous (IV) injections of 6.6 mg/kg paclitaxel (lot E046865AA; Hospira, Inc., Lake Forest, IL, USA) over 5 days.[19] This dose regimen equates to 118 mg/m^2 in humans and, as in patients, produces myelosuppression and decreases tumor growth in rats.[19,20] Control rats were injected intravenously with Kolliphor/ethanol/saline vehicle (KES), the vehicle for paclitaxel. A total of 110 rats were used in this study. Four were removed from the study due to phlebitis of the tail (2), death after paclitaxel injection (1), or gavage error (1). Numbers in each treatment group and experiment are provided in the figure legends.

Experimental Design

The first set of experiments (Fig. 1A) characterized the time course of paclitaxel-induced changes in the sensitivity of the cornea to tactile and chemical stimuli, as well as hypersensitivity of the hindpaw to tactile and cold stimuli. The second set of experiments (Fig. 1B) assessed the ability of NR to reverse the effects of paclitaxel in the cornea and the hindpaw. In addition to the behavioral measures, hindpaw tissue was taken from five rats in each group for determination of hindpaw IENF. Responsiveness to corneal application of capsaicin was also determined in a subset of these rats at the end of the experiment. The third set of experiments (Fig. 1C) assessed the effect of NR on tear production as well as responsiveness to capsaicin. Hindpaw tissue was also taken from five rats in each group for determination of hindpaw IENF. The final set of experiments assessed changes in the density of corneal afferents (Fig. 1D). This work was conducted in male rats because the effects of NR on paclitaxel-induced hypersensitivity of the hindpaw and IENF density had been determined earlier for female rats.[19,20] In that study, 200 mg/kg per os (PO) NR was an ED_{50} dose for reversal of established tactile hypersensitivity of the hindpaw; therefore, the dose for this study was increased to 500 mg/kg PO.[19] NR (ChromaDex, Irvine, CA, USA) was dissolved in water and administered by gavage (0.1 mL/100 g body weight) once daily for 28 days. The individuals conducting the behavioral, staining, or image analyses were not aware of treatment condition.

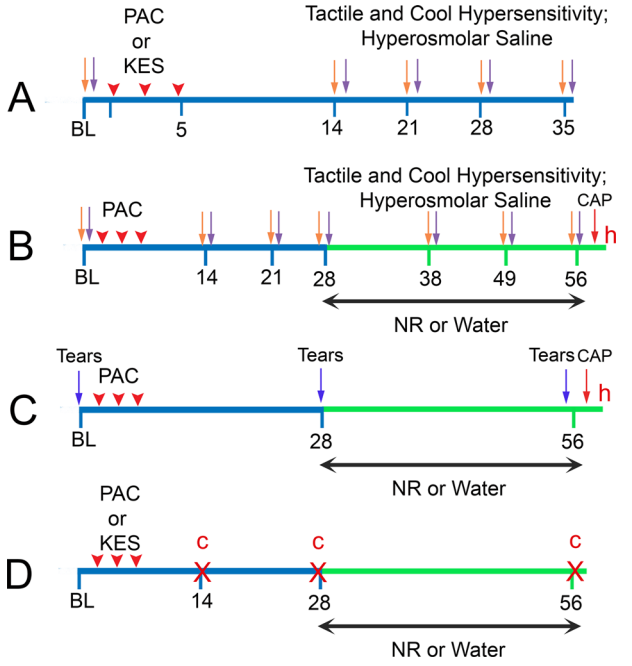

Figure 1. Schematic of experimental design for the four studies. (**A**) Characterization of time course of paclitaxel (PAC, *red arrowheads*)–induced hypersensitivity of the cornea to tactile stimuli (*orange arrows*) and hyperosmolar saline (*purple arrows*), as well as hindpaw to tactile and cool stimuli (*orange arrows*). (**B**) Characterization of ability of NR administration to reverse effects of paclitaxel. Capsaicin (CAP; 0.01% CAP) was also tested in a subset of rats. (**C**) Characterization of tear production and response to CAP in paclitaxel-treated rats with and without NR treatment (h) indicates euthanasia for measurement of IENF. (**D**) Illustration of time points at which rats were euthanized (X) to obtain cornea (c) for analysis of afferent density. KES is the vehicle for paclitaxel; water is the vehicle for NR.

Behavioral Measures

Rats were acclimated to the behavior testing room for 30 minutes and to the testing chambers for an additional 15 minutes.

Tactile Hypersensitivity. Withdrawal threshold to tactile stimulation of the hindpaw was determined using the Up-and-Down method.[21] Filaments corresponding to 1.1, 1.5, 2.2, 4.1, 5.7, 8.5, 10.1, 15.1, and 24.5 g were used; testing began with the 4.1-g filament. Rats that did not respond to the highest filament (i.e., paw was passively lifted by the filament) were assigned this value. The thresholds of the left and right paw were averaged to yield a single value for the rat. Paw withdrawal threshold values were transformed to their log value[22] to fulfill the statistical assumptions of a two-way repeated-measures analysis of variance (ANOVA) in which treatment was one factor and time was the repeated factor. Holm–Sidak's test was used for post hoc comparisons among group means. In this and all other repeated-measure ANOVAs, the Geisser–Greenhouse ε method was applied to correct for lack of sphericity on the time factor. A $P < 0.05$ was accepted for this and all other statistical analyses.

Cold Hypersensitivity. Rats were placed on an elevated glass surface. The barrel of a 3-cc syringe packed with dry ice was applied under the glass surface on which the hindpaw rested and withdrawal time was measured.[23] Values for each hindpaw were averaged to generate a single value for that rat. If withdrawal did not occur within

30 seconds, the test ended, and the rat was assigned this latency. Data were analyzed by two-way repeated-measures ANOVA in which treatment was one factor and time was the repeated factor. Holm–Sidak's test was used for post hoc comparisons among group means.

Coche–Bonnet Aesthesiometer. Rats were gently swaddled in a towel, in which a filament of the same diameter but different lengths ranging from 10 (most rigid, 10.3 g/mm^2) to 60 (least rigid, 0.4 g/mm^2) mm was applied perpendicular to the cornea (Luneau Ophthalmogie, Pont-de-l'Arche, France). The threshold force that elicited a withdrawal response was determined using the Up-and-Down method. Testing began with the filament extended to 40 mm; filament lengths of 60, 50, 40, 35, 30, 25, 20, 15, and 10 mm were used. Rats that did not blink or withdraw from the filament at the setting of 10 mm were assigned that force (termed *blink threshold*). Application of capsaicin or hyperosmolar saline to the cornea causes morphologic changes in corneal afferents.[24] For that reason, corneal withdrawal threshold values were determined only for the right eye so that the left eye could be used to assess chemical sensitivity. Values were log transformed to fulfill the statistical assumptions of a two-way repeated-measures ANOVA in which treatment was one factor and time was the repeated factor. Holm–Sidak's test was used for post hoc comparisons among group means. In the instance of missing values, a mixed-model ANOVA was used.

Chemical Stimuli. After acclimation to a pedestal in the middle of a brightly lit (450-lux) arena, rats were gently restrained and 10 µL hyperosmolar saline (Muro128 Solution 5%; 1710 mOsm/L; Bausch + Lomb, Bridgewater, NH, USA) was placed on the cornea of the left eye, after which the rat was immediately returned to the pedestal. Sensitivity to capsaicin (0.01%) was also evaluated on one occasion in one set of rats at the end of the study. The rat's behavior was videotaped for 3 minutes and then analyzed offline for the total number of wipes of the left eye with the ipsilateral frontpaw and squinting. For determination of squinting, the palpebral opening (height of the eye between upper and lower lids/length of the eye between canthi) was measured at 15, 45, 75, 105, 135, and 165 seconds and averaged to generate a single value for each rat. Instillation of hyperosmolar saline or capsaicin did not cause sustained closure of the eye. If observed at the time of analysis, the appropriate ratio was entered. During the study, the video camera was upgraded (60 frames/s), which enabled measurement of the number of blinks as well for a subset of rats. For hyperosmolar saline, data were analyzed by two-way repeated-measures ANOVA in which treatment was one factor and time was the repeated factor. As capsaicin was tested on only one occasion, a one-way ANOVA was used to test for differences among treatment groups.

Tearing. Rats were lightly anesthetized with isoflurane to assess basal tearing using Schirmer's test in which a strip of Whatman 41 filter paper (Cytiva, Marlborough, MA, USA) (1 mm wide and 17 mm long) was placed in the medial canthus of one eye. After 30 seconds, the strip was removed and the length of wetting was measured. Measurements were taken at baseline, 28 days after paclitaxel, and at the end of the 28-day treatment with NR. These measurements were made on a different day than the behavioral measures. Within-animal differences over time and differences between treatment groups were examined by a two-way repeated-measures ANOVA with Holm–Sidak's test for post hoc comparisons.

Immunohistochemistry

Rats were euthanized by CO_2 exposure followed by exsanguination. After enucleation, the aqueous humor was replaced with Zamboni's fixative containing 0.01% Triton X-100 and the eyeball immersed in Zamboni's fixative for 90 minutes. The cornea was then excised and immersed in Zamboni's fixative for another 2.5 hours. Corneas were rinsed twice for 15 minutes (0.05% Tween-20, 0.1 M phosphate-buffered saline pH 7.3 [PBS], 0.1 M glycine, and 0.1% sodium azide) and then incubated in a 1:1 mixture of Background Buster and Fc Receptor Block (Innovex Biosciences, Richmond, CA, USA) for 20 minutes, after which they were transferred to a blocking solution of 5% normal goat serum, 10% Fc Receptor Block, 10% Background Buster, 0.3% Triton X-100, 0.1 M PBS, 0.1 M glycine, and 0.1% sodium azide for 90 minutes at room temperature. Cornea were labeled for calcitonin gene-related peptide (CGRP) and neuronal class III β-tubulin by a stepwise protocol. Details of the antibodies are provided in the Table. All antibodies were diluted in PBS containing 5% normal goat serum, 0.3% Triton X-100, 0.1 M glycine, and 0.1% sodium azide. Corneas were incubated in polyclonal rabbit anti–α-CGRP overnight at 4°C. The following morning, the tissues were rinsed six times (10 minutes each) and incubated in Alexa 546 goat anti-

Table. Specifics of Antibodies

Antibodies	Source	Concentration, µg/mL	Catalog #	Lot #	RRID
Primary					
CGRP rabbit polyclonal whole serum	Immunostar (Hudson, WI, USA)	Cornea—1:4000 Skin—1:1000	24112	1714002	AB_572217
Tubulin β III mouse monoclonal IgG$_{2a}$	Biolegend (San Diego, CA, USA)	1	801202	B205807	AB_2313773
PGP 9.5 mouse monoclonal	EnCor Biotechnology (Gainesville, FL, USA)	1	MCA-BH7	120718	AB_2572394
Secondary					
Alexa Fluor 488 goat anti-mouse, IgG2a	Jackson ImmunoResearch (West Grove, PA, USA)	0.8	115-545-206	133801	AB_2338855
Alexa Fluor 546 goat anti-rabbit	Life Technologies (Carlsbad, CA, USA)	1	A11035	1904467	AB_2534093

Concentration: 1.88 µg/ml; donkey anti-mouse Cy3 (715–165-151, lot 132845); donkey anti-goat Cy2 (705–225-174, lot 1333888). They were purchased from Jackson ImmunoResearch (West Grove, PA).

Investigative Ophthalmology & Visual Science

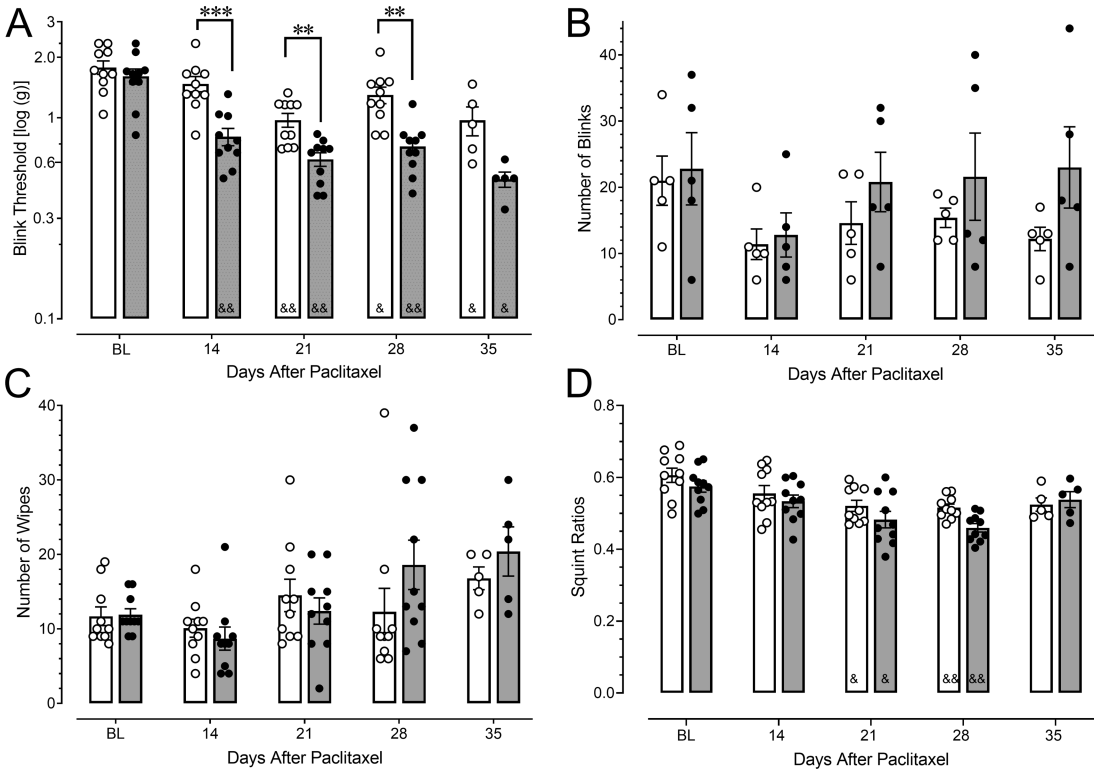

Figure 2. The effect of paclitaxel on the cornea is modality specific. (**A**) Decreased threshold for tactile stimulation. (**B–D**) The number of blinks and wipes and squinting (palpebral opening ratio) evoked by hyperosmolar saline is unchanged. Data are shown as scatterplots, with mean and SEM, and plotted as a function of time after the first injection of paclitaxel after baseline (BL) values were obtained. *Open circles* depict rats that received intravenous KES vehicle, with the mean represented by the *white bars*. *Filled circles* depict rats that received three injections of 6.6 mg/kg paclitaxel, with the mean represented by the *gray bars*. $n = 10$ except for $n = 5$ at 35 days for each treatment group. $^{**}P < 0.01$, $^{***}P < 0.001$ compared to KES-treated group at the corresponding time point. $^{\&}P < 0.05$, $^{\&\&}P < 0.01$ compared to BL within the treatment group. (**A**) Treatment, $F_{1, 18} = 25.60$; time, $F_{2.9, 45.4} = 38.44$; treatment × time, $F_{4, 62} = 4.53$. (**B**) Treatment, $F_{1, 18} = 1.37$; time, $F_{4, 32} = 2.63$; treatment × time, $F_{4, 32} = 0.79$. (**C**) Treatment, $F_{1, 18} = 0.56$; time, $F_{2.9, 45.4} = 4.22$; treatment × time, $F_{4, 62} = 1.82$. (**D**) Treatment, $F_{1, 18} = 2.99$; time, $F_{2.9, 45.7} = 15.27$; treatment × time, $F_{4, 62} = 0.82$.

rabbit IgG followed 1 hour later by mouse monoclonal anti–tubulin β3, IgG2a. The corneas were then incubated overnight at 4°C. After extensive rinsing, they were incubated in both secondary antibodies overnight at 4°C. Corneas were rinsed six times, slit through at four equidistant sides to flatten, cleared through an increasing series of glycerol, and mounted with Invitrogen Prolong Glass (Waltham, MA, USA).

A ~2-mm section of glabrous skin immediately caudal to the tori of the hindpaw was processed for protein gene product (PGP) 9.5 immunoreactivity (Table) as previously described[20] with several modifications. These modifications included processing the sections free-floating, increasing section thickness to 50 µm to better trace fibers, and inclusion of rabbit anti-CGRP with the anti-PGP antiserum to visualize peptidergic fibers.

Confocal Microscopy and Image Analysis

Corneal Nerve Density. Images were captured on either a Zeiss LSM 780 or LSM 900 confocal microscope with a 20 × 0.8 NA M27 Plan-Apochromat objective (Carl Zeiss MicroImaging, Thornwood, NY, USA). Corneal images were taken from the central cornea and included the whorl-like vortex as an anchor. Z-stacks bounded by the vertical extent of β-tubulin and CGRP immunoreactivity were captured using the single-pass, multitracking format. Confocal image sizes in the x and y planes were the same for every image (2048 × 2048 pixels). The image sizes in the z plane were different as we had to accommodate the natural variation in corneal epithelium thickness. Variation in the z plane was corrected by isolating the corneal epithelium labeling from the rest of the image (see below).

Corneal nerve fiber density analysis was performed as described.[24] Analysis was performed using Imaris 9.1 software (Bitplane USA, Concord, MA, USA; RRID: SCR_007370) on an offline workstation in the Advanced Light Microscopy Core at Oregon Health & Science University (OHSU). Corneal nerve density was defined as the density of the subbasal and intraepithelial corneal nerves taken together. To correct for variation in the z plane of each confocal scan and avoid including stromal nerve labeling, the Surfaces segmentation tool was used to manually isolate the corneal epithelium from the rest of the image, and a surface was created that served as a region of interest (ROI) for the rest of the analysis. The volume of the corneal epithelium ROI was calculated by the software. The Mask Channel function was then used to isolate β-tubulin and CGRP labeling within the corneal epithelium ROI for further analysis.

β-Tubulin labeling within the ROI was thresholded using the Surfaces segmentation tool and a volume (μm^3) was

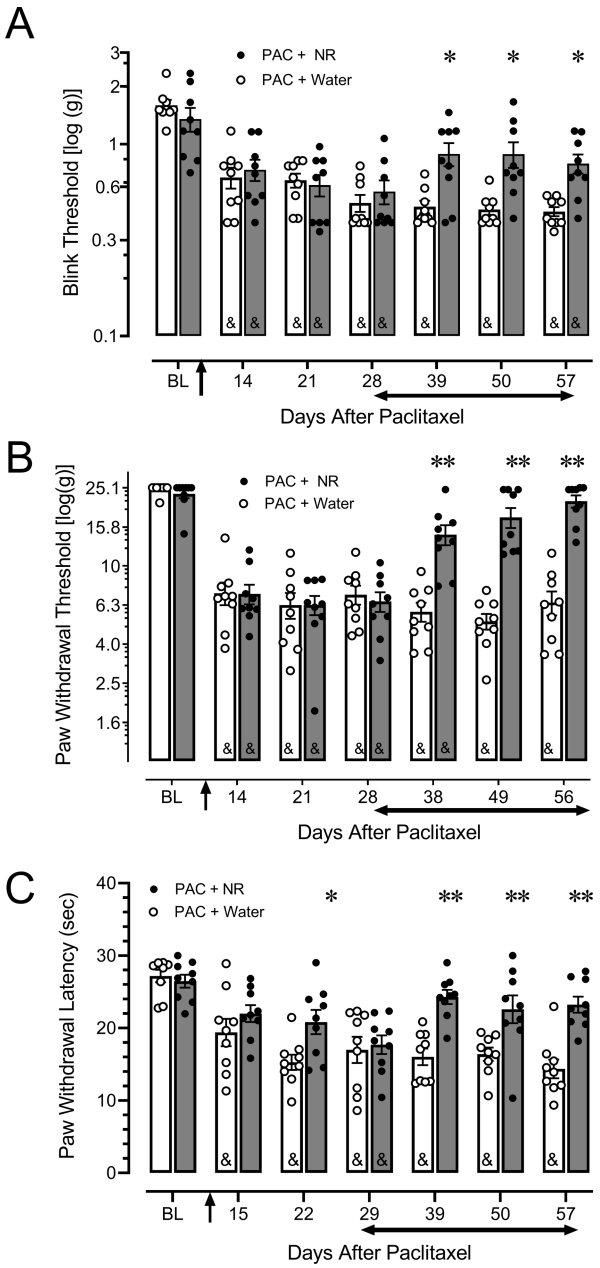

Figure 3. NR reverses paclitaxel-induced (**A**) tactile hypersensitivity of the cornea, as well as (**B**) tactile and (**C**) cool hypersensitivity of the hindpaw in male rats. After baseline (BL) measurements, rats received three intravenous injections of 6.6 mg/kg paclitaxel over 5 days (*arrows*). *Horizontal line* indicates daily oral administration of 500 mg/kg NR, beginning 4 weeks later. Data are scatterplots of individual rats, with *bars* illustrating the mean and SEM. *Filled circles* depict rats that received paclitaxel + NR, with the mean represented by the *gray bars*. *Open circles* depict rats that received paclitaxel + water, with the mean represented by the *white bars*. $^{*}P < 0.05$, $^{**}P < 0.01$ compared to paclitaxel + water-treated group at the corresponding time point. $^{\&}$Significant difference from BL of at least $P < 0.05$. $n = 9$ for each group. (**A**) Treatment, $F_{1,\ 16} = 4.64$; time, $F_{4.2,\ 67.3} = 26.71$; treatment × time, $F_{6,\ 96} = 6.66$. (**B**) Treatment, $F_{1,\ 16} = 21.92$; time, $F_{4.1,\ 66.2} = 47.63$; treatment × time, $F_{6,\ 96} = 20.47$. (**C**) Treatment, $F_{1,\ 16} = 41.55$; time, $F_{4.3,\ 68.1} = 11.03$; treatment × time, $F_{6,\ 96} = 3.83$.

calculated. The β-tubulin volume was expressed as the percentage of the epithelium that contained β-tubulin–labeled nerves (% β-tubulin). To measure changes in CGRP specifically within corneal nerves, the β-tubulin volume was established as the ROI, and the Mask Channel function was used to further determine CGRP labeling within β-tubulin–labeled nerves. The labeling for each marker was thresholded separately and the volume of CGRP (μm^3) was calculated. As above, the CGRP volume within the β-tubulin ROI of each cornea was normalized to the corneal epithelium volume and expressed as % CGRP (or the percentage of the epithelium that contained CGRP-labeled corneal nerves). Values from the left and right corneas were averaged to generate one value for each rat. One-way ANOVA followed by Holm–Sidak's test was used to compare treatment group means.

Methodologic Considerations

The confocal microscope used for scanning corneas was upgraded from a Zeiss LSM 780 to a Zeiss LSM 900 midway through the corneal nerve density studies. Efforts were made to keep scanning parameters the same when possible, but there were differences in image size due to an increase in the quality of pixel resolution with the new system. Consequently, a 2048 × 2048 scan on the new system was smaller (0.223 × 0.223 µm) than the earlier scans taken with the older system (0.297 × 0.297 µm). Differences in epithelial volumes were accounted for by multiplying epithelial volumes taken with the older system by a factor of 0.564.

We used a protocol combining immunocytochemical methods and confocal microscopy with advanced imaging tools for assessing corneal nerve density and neurochemical composition as previously described.[24] By using advanced imaging tools, we compensated for variations in z-thickness and avoided the confounds of stromal nerve labeling, thereby limiting our analyses specifically to the corneal epithelium. We calculated volumes for each marker as a portion of the epithelium volume for each cornea to allow between-animal or between-treatment comparisons, so that potential differences found in the different markers are not attributable to differences in epithelium volume.

Intraepidermal Nerve Fibers in the Hindpaw. Five rats were randomly selected from the 10 rats in each treatment group for analysis. The number of IENF crossings at the epidermal–dermal border of the hindpaw was counted in five to six sections from each rat using StereoInvestigator (MBF Biosciences, Williston, VT, USA) as previously described.[20] Numbers of fibers were normalized to the length of the border in each section and then averaged to yield a single value for that rat. Langerhans cells, which are also immunoreactive for PGP 9.5 and identified by their spindle or stellate shape with extensive processes, were counted as well and normalized to the volume of tissue that was examined. Data were analyzed by one-way ANOVA followed by Holm–Sidak's test.

Results

Paclitaxel Treatment Evoked Modality-Specific Hypersensitivity to Corneal Stimulation

Although repeated testing itself caused a progressive increase in tactile hypersensitivity of the cornea in vehicle-treated rats, the magnitude of tactile hypersensitivity was

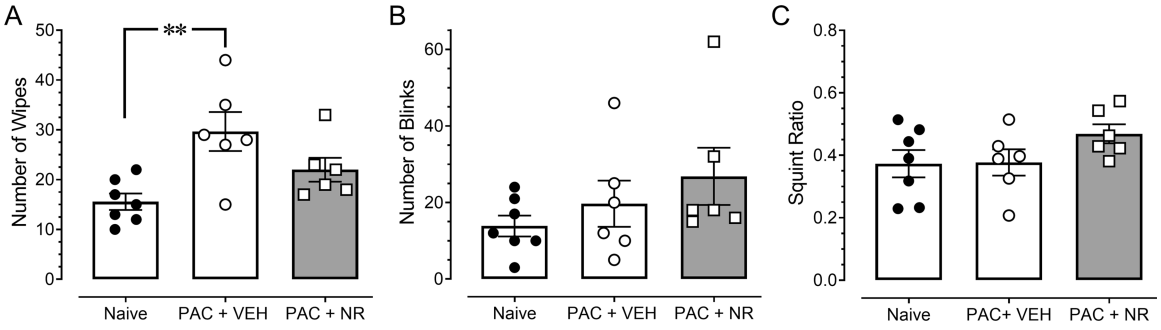

Figure 4. Number of (**A**) eye wipes but not (**B**) blinks evoked by 0.01% capsaicin is increased in paclitaxel-treated rats. Squint ratio (**C**) is unaffected. Rats were tested 56 to 58 days after paclitaxel. Panels are scatterplots of data from individual rats ($n = 6$ in each treatment group). Bars indicate mean ± SEM Historical, unpublished data from seven naive rats are included. $^{**}P < 0.01$ compared to naive rats. (**A**) $F_{2, 16} = 6.892$. (**B**) $F_{2, 16} = 1.413$. (**C**) $F_{2, 16} = 1.784$.

consistently greater in paclitaxel-treated rats (Fig. 2A). Tactile hypersensitivity was evident as early as 14 days after paclitaxel treatment began and persisted through 28 days. In contrast, paclitaxel treatment did not enhance responsiveness of the cornea to hyperosmolar saline as measured by the number of wipes, blinks, or squint ratio (Figs. 2B–D).

NR Treatment Reversed Established Hypersensitivity of Both Cornea and Hindpaw

NR reversed paclitaxel-induced tactile hypersensitivity of the cornea (Fig. 3A). It also reversed established hypersensitivity to both tactile and cool stimulation of the hindpaw in male rats (Figs. 3B, 3C; $P < 0.001$ for both), as it did in female rats.[19,20] NR did not affect blinking, wiping, or squint ratio after application of hyperosmolar saline (data not shown). Responsiveness to corneal application of 0.01% capsaicin was therefore tested in a small subset of rats from this experiment. Based on these pilot results (not illustrated), an additional cohort of 12 rats was run to prospectively evaluate effects of NR on capsaicin responsiveness and to also determine the effects of paclitaxel treatment on tear production (Fig. 1C). Capsaicin was tested only once at 56 to 58 days, and these rats did not undergo any testing other than a modified Schirmer's test at 28 and 56 days. Figure 4A illustrates that when assessed 56 to 58 days after paclitaxel treatment, capsaicin caused a nearly twofold increase in the number of wipes compared to naive rats ($P = 0.006$). The number of blinks and squint ratio were unchanged (Figs. 4B, 4C; $P = 0.7$ and 0.94, respectively). Tear production was increased 28 days after paclitaxel treatment (9.3 ± 0.6 mm) compared to baseline (6.3 ± 0.2 mm, $n = 12$; $P < 0.005$). Treatment with NR also did not modify capsaicin-induced blinking and squinting (Figs. 4B, 4C). It had an indeterminate effect on the exaggerated wipe response (Fig. 4A), in that the NR-treated group did not differ from the water-treated group ($P = 0.19$), yet also did not differ from naive rats ($P = 0.29$). Tear production remained increased 56 days after paclitaxel treatment in rats that received water (10.6 ± 1.0 mm) or NR (11.4 ± 1.0 mm; $n = 6$ each group); these groups did not differ ($P = 0.37$).

Paclitaxel Does Not Cause Sustained Loss of Corneal Afferents

We tested whether paclitaxel treatment causes a loss of innervation in the corneal epithelium at 28 or 56 days after treatment. To ensure that changes in innervation are not due to overall structural changes in the epithelium, we examined total epithelial volume as well as nerve density. Epithelial volume (Fig. 5A; $P = 0.96$; $F_{5, 28} = 0.19$) did not differ among untreated naive rats, in either group of rats that received paclitaxel vehicle (i.e., KES), or in rats 14, 28, or 56 days

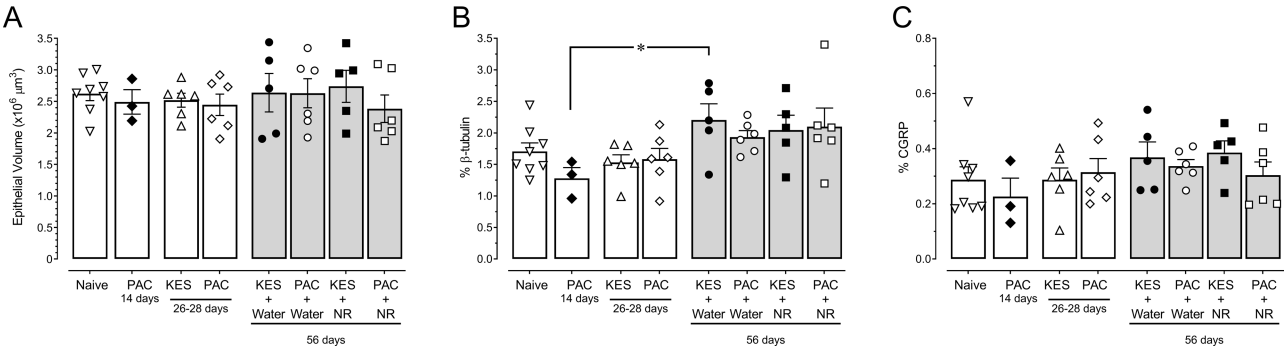

Figure 5. Paclitaxel does not alter (**A**) epithelial volume or the density of (**B**) β-tubulin immunoreactivity or (**C**) CGRP immunoreactivity in the cornea. Data for β-tubulin and CGRP are expressed as a percentage of epithelial volume. *Bars* depict mean ± SEM. Panels are a scatterplot of values from individual rats euthanized 26 to 28 days or 56 days after the first of three intravenous injections of KES vehicle or 6.6 mg/kg PAC with or without treatment with nicotinamide riboside. Also depicted are values from naive rats housed with the cohort and rats euthanized 14 days after paclitaxel. $^{*}P < 0.05$. $n = 3$–8 in each treatment group. (**A**) $F_{7, 37} = 0.344$. (**B**) $F_{7, 37} = 2.261$; (**C**) $F_{7, 37} = 0.8836$.

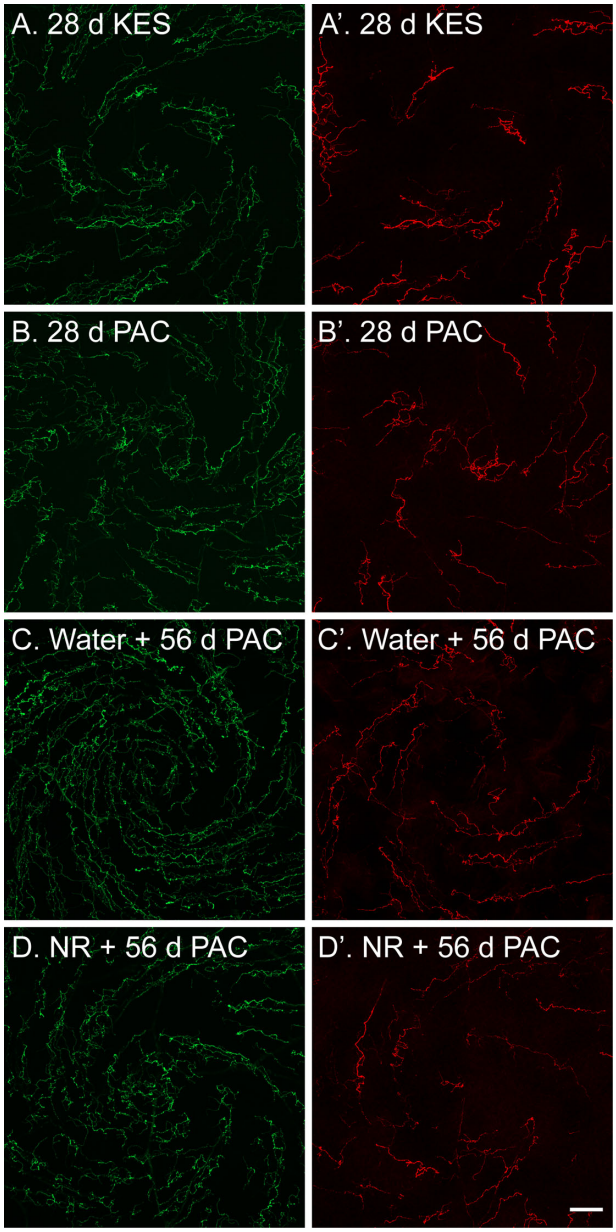

Figure 6. Representative confocal micrographs of immunolabeling for β-tubulin (*green*; **A–D**) or CGRP (*red*; **A′–D′**) in corneas obtained from rats 26 to 28 days after intravenous (IV) treatment with KES (**A**, **A′**) or paclitaxel (PAC; **B**, **B′**). (**C**, **D**) Cornea from rats 56 days after intravenous administration of paclitaxel and either 4 weeks' treatment with water (**C**, **C′**) or NR (**D**, **D′**), which commenced 28 days after paclitaxel. *Scale bar*: 50 µm. Confocal micrographs are maximum-intensity projections of optical slices containing corneal nerves in the epithelial and subbasal layers of the cornea. Images were adjusted for optimal brightness and contrast using Zeiss Zen software.

after paclitaxel treatment. Similarly, the density of β-tubulin immunoreactive fibers did not differ with the sole exception of the 14-day paclitaxel treatment group, which was transiently reduced compared to the 56-day KES + vehicle treatment group (Fig. 5B; $P = 0.02$; $F_{5,\ 28} = 3.18$). The density of CGRP-immunoreactive fibers did not differ among any of these treatment groups (Fig. 5C; $P = 0.57$; $F_{5,\ 28} = 0.78$). Treatment with NR had no additional effects on any corneal epithelial parameters. Representative images of immunostaining for β-tubulin or CGRP in the cornea at 26 to 28 days or 56 days after paclitaxel with or without NR are presented in Figure 6.

NR Does Not Reverse Paclitaxel-Induced Loss of IENF in the Hindpaw

The density of hindpaw IENF 56 days after paclitaxel treatment was approximately half that of saline-treated controls (Fig. 7A; $P = 0.012$). Fibers that persisted appeared of finer caliber and stained with weaker intensity. IENF density in the hindpaw of paclitaxel-treated rats that received NR did not differ from that of the vehicle-treated cohort ($P = 0.415$) and was also not significantly different from saline-treated controls ($P = 0.139$). In contrast, the average density of CGRP-immunoreactive fibers in the hindpaw did not differ among saline-treated controls and either group of paclitaxel-treated rats (Fig. 7B; $P = 0.14$). Given that these afferents are a subset of those that stain for PGP 9.5 and a loss of PGP 9.5 fibers occurred in paclitaxel-treated rats, these data were normalized to the number of PGP 9.5–positive fibers. This transformation revealed that the percentage of PGP 9.5–positive fibers that were CGRP immunoreactive was significantly increased in paclitaxel-treated rats that received vehicle (Fig. 7C; $P = 0.033$) or NR ($P = 0.017$) compared to saline-treated controls; the paclitaxel-treated groups did not differ from one another ($P = 0.97$). This finding suggests that paclitaxel may cause a preferential loss of nonpeptidergic afferents. The number of Langerhans cells in paclitaxel-treated rats that received vehicle did not differ from the NR-treated cohort ($P = 0.48$) or saline-treated controls ($P = 0.56$). However, paclitaxel-treated rats that received NR exhibited significantly more Langerhans cells than saline-treated controls (Fig. 7D; $P = 0.048$). Representative images of hindpaw IENF in vehicle- and NR-treated rats are provided in Figure 8.

Discussion

Paclitaxel treatment produces sustained tactile hypersensitivity of the cornea, increased tear production, and enhanced responsiveness to corneal application of capsaicin; it does not exacerbate responsiveness to corneal application of hyperosmolar saline. These findings suggest that paclitaxel in the rodent could serve as a model of chemotherapy-induced ocular discomfort. Although the increase in tear production appears counterintuitive, ocular discomfort and DES can occur independent of a deficit in tear production. Other factors such as tear composition, stability, and viscosity can be contributing factors.[4–6] Nonetheless, in the absence of other conventional diagnostic criteria (e.g., interruption of tear film integrity or increased osmolarity), the increase in tearing cautions against characterization of paclitaxel as a model of DES. In contrast, surgical excision of the lacrimal glands produces a tear deficit,[25–28] tactile hypersensitivity,[29] and hypersensitivity to hyperosmolar saline and capsaicin.[30,31] Corneal abrasion by application of heptanol causes a short-lived heightened sensitivity to menthol followed 1 week later by a tear deficit in male rats.[32] It is also possible that the increased tearing reflects ongoing nociceptor activation. Unfortunately, basal squint ratio and blinking were not recorded before instillation of hyperosmolar saline or capsaicin. Finally, the magnitude of squinting induced by Muro-128 was less than anticipated based on a

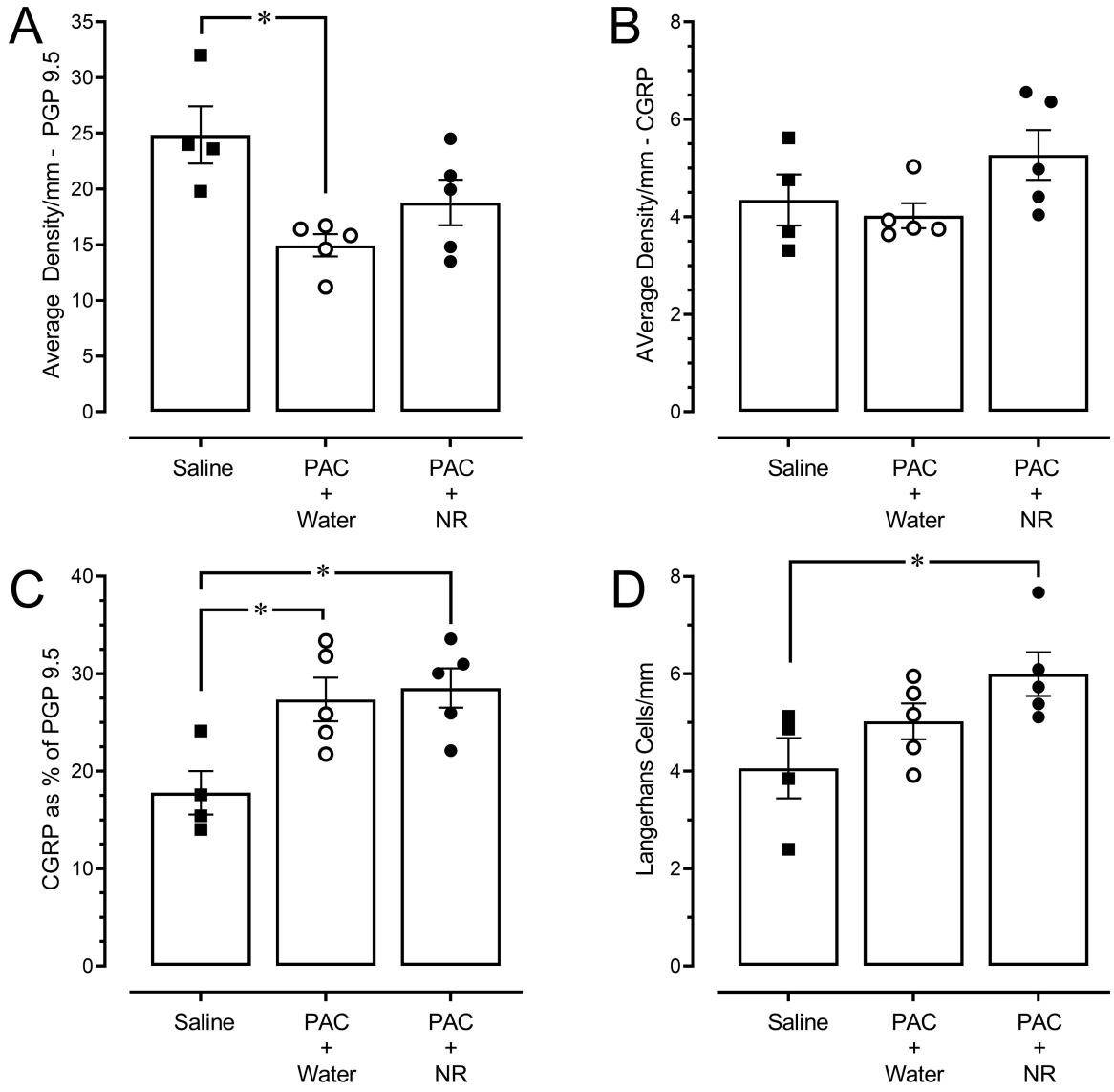

Figure 7. Paclitaxel causes a sustained loss of hindpaw IENFs as visualized by PGP 9.5 immunoreactivity (**A**) but not peptidergic fibers as visualized by CGRP (**B**). Normalization of CGRP fibers to PGP 9.5 fibers (**C**) reveals that paclitaxel may cause a preferential loss of nonpeptidergic fibers. Treatment with 500 mg/kg NR daily for 28 days did not reverse the loss of hindpaw IENF. However, NR treatment was associated with a significant increase in number of Langerhans cells (**D**). Panels are a scatterplot of values from individual rats euthanized 56 days after the first injection of paclitaxel and treated with water or 500 mg/kg NR beginning at 28 days. *Bars* indicate mean ± SEM. n = 5 in each group and 4 for rats that received only intravenous saline. *$P < 0.05$. (**A**) $F_{2, 11} = 2.326$. (**B**) $F_{2, 11} = 6.767$. (**C**) $F_{2, 11} = 4.042$.

prior report[33] but may reflect dilution of the hyperosmolar saline due to increased basal tearing.

Studies of sex differences have reported that female rats and mice exhibit a more robust response to excision of the lacrimal gland than males.[34,35] The lack of response to hyperosmolar saline in our present study may therefore be a function of sex rather than model. As observed in female rats,[19,20] paclitaxel also produced sustained hypersensitivity to tactile and cool stimulation of the hindpaw in male rats.

Paclitaxel-induced tactile hypersensitivity of the cornea occurred in the absence of overt changes in the density of corneal afferents as visualized by β-tubulin or CGRP immunoreactivity either in the period shortly after injury (14 days) or as late as 8 weeks out. This finding was unexpected because the density of β-tubulin immunoreactive corneal afferents is reportedly reduced 2 weeks after a single intraperitoneal injection of 10 to 20 mg/kg paclitaxel in male mice.[36] That report aside, the density of $Na_V1.8$-expressing corneal afferents in male and female mice was unchanged in the lacrimal gland excision model of DES.[35] Paclitaxel-treated rats also exhibited an enhanced response to capsaicin. Lacrimal gland excision, which increases responsiveness to capsaicin, is associated with increased transient receptor potential cation channel subfamily V member 1 (TRPV1) expression in trigeminal ganglion neurons.[30,37] Although the enhanced sensitivity to capsaicin that we observed suggests that paclitaxel may similarly increase TRPV1 expression in corneal afferents, methodologic issues, including an increase in diffuse "background" labeling coupled with the small numbers of TRPV1-immunolabeled afferents, prevented reliable quantitation of TRPV1-immunoreactive fibers in the cornea of KES- or paclitaxel-treated rats.

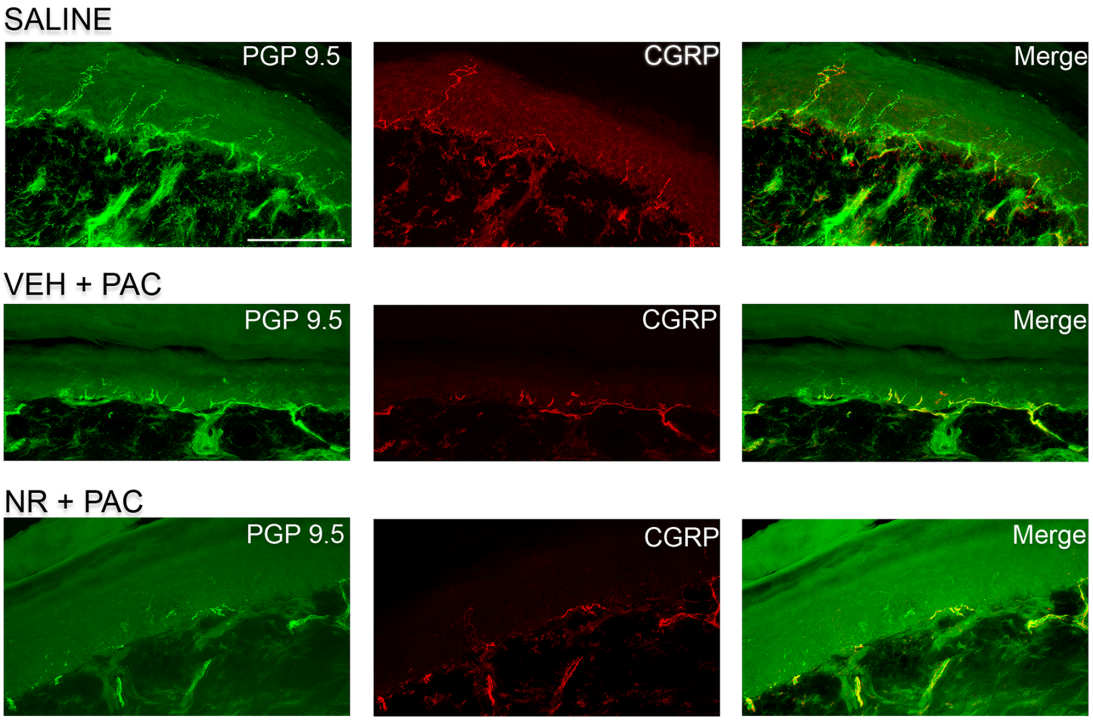

Figure 8. Representative confocal micrographs of immunolabeling for PGP 9.5, CGRP, and merged channels in glabrous skin of the hindpaw of rats 56 days after intravenous administration of paclitaxel and 28 days treatment with vehicle or NR. *Top* panels were taken from male rats that received intravenous saline. *Scale bar*: 100 microns. Each image is a maximum-intensity projection of 15 to 18 optical sections that, in the interest of publication, were adjusted for optimal brightness and contrast using Photoshop software (Adobe, San Jose, CA, USA).

At first glance, the preservation of corneal afferents in paclitaxel-treated rats appears to run counter to the findings of a recent cross-sectional study.[9,13,38] However, methodologic differences are a likely factor. The cross-sectional study in patients used in vivo confocal microscopy, which images the subbasal nerve plexus, whereas this study examined nerve endings in the corneal epithelium. Patients in that study had received between 7 and 12 cycles of chemotherapy (roughly 7 to 12 months of therapy). Rats in this study received three injections within 5 days, which suppressed tumor growth through day 9[20] and is analogous to a single infusion. Finally, even among those patients reporting peripheral neuropathy, corneal nerve density was reduced by only ~24%.[9] Injury is known to cause sprouting.[39,40] It is possible that the density of nerves in the subbasal plexus is diminished, yet remaining axons that enter the corneal epithelium sprout after the injury. Corneal epithelium and stromal nerves can reinnervate in the presence of a persistent decrease in the density of the subbasal nerve plexus[40] and references therein. Indeed, direct reinnervation of the epithelium from stromal nerves has been documented.[39] Finally, our focus on the central area may have limited our ability to detect changes. In patients receiving platinum-based chemotherapy, the density of the subbasal nerve plexus in the central area was unaffected yet was decreased in the inferior whorl.[13] Chemotherapy-induced peripheral neuropathy frequently localizes to the feet and hands with a stocking- and glove-like distribution. This pattern has been attributed to the greater metabolic needs and therefore enhanced vulnerability of primary afferent neurons with long axons.[41] Although attractive, this idea may need to be rethought. First, only the glabrous skin and not the dorsal hairy skin of the rat hindpaw exhibits mechanical hypersensitivity after paclitaxel treatment, suggesting that axon length is not a factor in the occurrence of peripheral neuropathy in the distal extremities.[42] Second, tactile hypersensitivity of the cornea and the hindpaw developed in parallel in this study despite large differences in the length of axons that innervate the cornea and the hindpaws. Histologic analyses demonstrated a loss of IENF in the hindpaw after paclitaxel, which is consistent with previous studies.[14,20,43] However, paclitaxel did not decrease the density of corneal nerve fibers in the epithelium. To the best of our knowledge, only one other study has assessed the effects of paclitaxel on the density of corneal nerve fibers in the rodent. That study reported a decrease in corneal nerve fiber density that paralleled that in the hindpaw.[36] The basis for the different findings in the cornea is unclear, but several possibilities can be entertained. Corneal afferents in the rat may be more resistant to paclitaxel. Although this dose regimen causes myelosuppression, decreases tumor growth, and reduces hindpaw IENF,[19,20] it may be insufficient for the cornea. The avascular nature (i.e., angiogenic privilege) of the cornea may be a fundamental factor.[44] Several laboratories have recently identified the axon and peripheral nerve endings—and not the cell soma—as sites of action of paclitaxel.[45–47] If paclitaxel is unable to readily access the peripheral endings of corneal afferents, it may not cause terminal arbor degeneration. Similarly, if a direct effect on peripheral nerve endings contributes to the ability of NR to reverse tactile hypersensitivity, then the avascular nature of the cornea could limit its efficacy.

Tactile hypersensitivity of the cornea occurred in the absence of any apparent loss of afferent innervation, whereas this was not the case for the hindpaw. This disparity suggests that loss of afferent innervation is not

a prerequisite for paclitaxel-induced tactile hypersensitivity. It also suggests that NR suppression of corneal hypersensitivity is independent of changes in corneal innervation, although it does not exclude normalization or an upregulation of receptors or channels such as Piezo2 or TRPV1 on afferent endings or suppression of inflammatory cells. With respect to the hindpaw, pretreatment with 200 mg/kg NR can prevent the loss of hindpaw IENF in female rats.[20] Here, NR was unable to convincingly reverse established loss of IENF in the hindpaw of male rats despite administration of a more than twofold higher dose of NR. This finding similarly points to additional mechanisms of action that are independent of terminal arbor degeneration.

The preservation of nociceptive responses in dermatomes that have undergone persistent loss of hindpaw IENF is a conundrum. The finding that the loss may occur preferentially in nonpeptidergic fibers provides a new perspective. Additional support is provided by an earlier study in which paclitaxel caused only a modest decrease in CGRP-immunoreactive IENF in the hindpaw.[48] Normalizing those data to the number of PGP 9.5–positive IENF that remained, as done here, reveals a similar preferential preservation of CGRP-immunoreactive afferents. Interestingly, paclitaxel increases the expression of Nav1.7 in small- to medium-diameter isolectin B4–positive as well as CGRP-positive neurons of the dorsal root ganglia, but particularly so in the CGRP-positive population.[49,50]

In summary, paclitaxel treatment induced sustained, modality-specific hypersensitivity of the cornea and increased tear production. These actions were independent of changes in corneal innervation, suggesting that loss of corneal afferent innervation is not a prerequisite for corneal hypersensitivity. As anticipated, paclitaxel also produced hypersensitivity of the hindpaw to tactile and cool stimuli in male rats. Daily administration of NR was able to reverse tactile hypersensitivity of the cornea, as well as tactile and cool hypersensitivity of the hindpaw. These findings suggest that patients experiencing ocular discomfort as a result of chemotherapy may experience relief with this natural product and isoform of vitamin B3. The exact mechanism by which NR reverses corneal discomfort and somatic hypersensitivity is not yet fully understood. Although the hypothesis that its neuroprotective effects are due to correction of mitochondrial dysfunction and increases in NAD^+ remains attractive,[19,20] recent clinical trials hint at possible anti-inflammatory mechanisms.[51,52] The finding that NR reversed hypersensitivity of the hindpaw without reversing the loss of hindpaw IENF suggests that restoration of afferent innervation is not central to the effects of NR in the therapeutic setting.

Acknowledgments

The authors thank Randy Kardon for support and insights he shared, Pieter Poolman for development of the 360° video monitoring system, Elizabeth Birchfield for many hours spent analyzing videotaped behaviors, and ChromaDex for providing NR gratis.

Supported by R01AT009705, by a pilot award from the Center for Prevention and Treatment of Visual Loss to DLH, and by P30NS061800 to SAA.

Disclosure: **M.V. Hamity**, ChromaDex (F); **S.J. Kolker**, None; **D.M. Hegarty**, None; **C. Blum**, None; **L. Langmack**, None; **S.A. Aicher**, None; **D.L. Hammond**, ChromaDex (F)

References

1. Stapleton F, Alves M, Bunya VY, et al. TFOS DEWS II epidemiology report. *Ocul Surf*. 2017;15:334–365.
2. Kalangara JP, Galor A, Levitt RC, Felix ER, Alegret R, Sarantopoulos CD. Burning eye syndrome: do neuropathic pain mechanisms underlie chronic dry eye? *Pain Med*. 2016;17:746–755.
3. Mehra D, Cohen NK, Galor A. Ocular surface pain: a narrative review. *Ophthalmol Ther*. 2020;9:1–21.
4. Meng ID, Kurose M. The role of corneal afferent neurons in regulating tears under normal and dry eye conditions. *Exp Eye Res*. 2013;117:79–87.
5. Belmonte C, Nichols JJ, Cox SM, et al. TFOS DEWS II pain and sensation report. *Ocul Surf*. 2017;15:404–437.
6. Labetoulle M, Baudouin C, Calonge M, et al. Role of corneal nerves in ocular surface homeostasis and disease. *Acta Ophthalmol*. 2019;97:137–145.
7. Hosotani Y, Ishikawa H, Mihanaga K, Gomi F. Anti-cancer drug nab-paclitaxel may exacerbate corneal epithelial disorder. *J Clin Case Rep*. 2017;7:1002.
8. Lee HS, Ha JY, Choi W, Yoon KC. Bilateral corneal epithelial lesions associated with paclitaxel. *Optom Vis Sci*. 2016;93:1333–1336.
9. Chiang JCB, Goldstein D, Trinh T, et al. A cross-sectional study of ocular surface discomfort and corneal nerve dysfunction after paclitaxel treatment for cancer. *Sci Rep*. 2021;11:1786.
10. Sagga N, Kuffova L, Vargesson N, Erskine L, Collinson JM. Limbal epithelial stem cell activity and corneal epithelial cell cycle parameters in adult and aging mice. *Stem Cell Res*. 2018;33:185–198.
11. Katikireddy KR, Schmedt T, Price MO, Price FW, Jurkunas UV. Existence of neural crest-derived progenitor cells in normal and Fuchs endothelial dystrophy corneal endothelium. *Am J Pathol*. 2016;186:2736–2750.
12. Yam GH, Seah X, Yusoff N, et al. Characterization of human transition zone reveals a putative progenitor-enriched niche of corneal endothelium. *Cells*. 2019;8:1244.
13. Chiang JCB, Goldstein D, Trinh T, et al. A cross-sectional study of sub-basal corneal nerve reduction following neurotoxic chemotherapy. *Transl Vis Sci Technol*. 2021;10:24.
14. Bennett GJ, Liu GK, Xiao WH, Jin HW, Siau C. Terminal arbor degeneration—a novel lesion produced by the antineoplastic agent paclitaxel. *Eur J Neurosci*. 2011;33:1667–1676.
15. Bieganowski P, Brenner C. Discoveries of nicotinamide riboside as a nutrient and conserved NRK genes establish a Preiss-Handler independent route to NAD^+ in fungi and humans. *Cell*. 2004;117:495–502.
16. Trammell SAJ, Schmidt MS, Weidemann BH, et al. Nicotinamide riboside is uniquely bioavailable in mouse and man. *Nature Comm*. 2016;7:14298.
17. Trammell SA, Weidemann BJ, Chadda A, et al. Nicotinamide riboside opposes type 2 diabetes and neuropathy in mice. *Sci Rep*. 2016;6:26933.
18. Brown KD, Maqsood S, Huang JY, et al. Activation of SIRT3 by the NAD^+ precursor nicotinamide riboside protects from noise-induced hearing loss. *Cell Metab*. 2014;20:1059–1068.
19. Hamity MV, White SR, Walder RY, Schmidt MS, Brenner C, Hammond DL. Nicotinamide riboside, a form of vitamin B3 and NAD^+ precursor, relieves the nociceptive and aversive dimensions of paclitaxel-induced peripheral neuropathy in female rats. *Pain*. 2017;158:962–972.
20. Hamity MV, White SR, Blum C, Gibson-Corley KN, Hammond DL. Nicotinamide riboside relieves paclitaxel-induced peripheral neuropathy and enhances suppression of tumor growth in tumor-bearing rats. *Pain*. 2020;161:2364–2375.

21. Chaplan SR, Bach FW, Pogrel JW, Chung JM, Yaksh TL. Quantitative assessment of tactile allodynia in the rat paw. *J Neurosci Methods*. 1994;53:55–63.
22. Mills C, Leblond D, Joshi S, et al. Estimating efficacy and drug ED50's using von Frey thresholds: impact of Weber's law and log transformation. *J Pain*. 2012;13:519–523.
23. Brenner DS, Golden JP, Gereau RW. A novel behavioral assay for measuring cold sensation in mice. *PLoS One*. 2012;7:e39765.
24. Hegarty DM, Hermes SM, Yang K, Aicher SA. Select noxious stimuli induce changes on corneal nerve morphology. *J Comp Neurol*. 2017;525:2019–2031.
25. Shinomiya K, Ueta M, Kinoshita S. A new dry eye mouse model produced by exorbital and intraorbital lacrimal gland excision. *Sci Rep*. 2018;8:1483.
26. Stevenson W, Chen Y, Lee SM, et al. Extraorbital lacrimal gland excision: a reproducible model of severe aqueous tear-deficient dry eye disease. *Cornea*. 2014;33:1336–1341.
27. Mecum NE, Cyr D, Malon J, Demers D, Cao L, Meng ID. Evaluation of corneal damage after lacrimal gland excision in male and female mice. *Invest Ophthalmol Vis Sci*. 2019;60:3264–3274.
28. Joossen C, Lanckacker E, Zakaria N, et al. Optimization and validation of an existing, surgical and robust dry eye rat model for the evaluation of therapeutic compounds. *Exp Eye Res*. 2016;146:172–178.
29. Fakih D, Zhao Z, Nicolle P, et al. Chronic dry eye induced corneal hypersensitivity, neuroinflammatory responses, and synaptic plasticity in the mouse trigeminal brainstem. *J Neuroinflammation*. 2019;16:268.
30. Bereiter DA, Rahman M, Thompson R, Stephenson P, Saito H. TRPV1 and TRPM8 channels and nocifensive behavior in a rat model for dry eye. *Invest Ophthalmol Vis Sci*. 2018;59:3739–3746.
31. Meng ID, Barton ST, Mecum NE, Kurose M. Corneal sensitivity following lacrimal gland excision in the rat. *Invest Ophthalmol Vis Sci*. 2015;56:3347–3354.
32. Hegarty DM, Hermes SM, Morgan MM, Aicher SA. Acute hyperalgesia and delayed dry eye after corneal abrasion injury. *Pain Rep*. 2018;3:e664.
33. Yorek MS, Davidson EP, Poolman P, et al. Corneal sensitivity to hyperosmolar eye drops: a novel behavioral assay to assess diabetic peripheral neuropathy. *Invest Ophthalmol Vis Sci*. 2016;57:2412–2419.
34. Skrzypecki J, Tomasz H, Karolina C. Variability of dry eye disease following removal of lacrimal glands in rats. *Med Sci Res*. 2019;1153:109–115.
35. Mecum NE, Demers D, Sullivan CE, Denis TE, Kalliel JR, Meng ID. Lacrimal gland excision in male and female mice causes ocular pain and anxiety-like behaviors. *Sci Rep*. 2020;10:17225.
36. Ferrari G, Nallasamy N, Downs H, Dana R, Oaklander AL. Corneal innervation as a window to peripheral neuropathies. *Exp Eye Res*. 2013;113:148–150.
37. Hatta A, Kurose M, Sullivan C, et al. Dry eye sensitizes cool cells to capsaicin-induced changes in activity via TRPV1. *J Neurophysiol*. 2019;121:2191–2201.
38. Chiang JCB, Goldstein D, Park SB, Krishnan AV, Markoulli M. Corneal nerve changes following treatment with neurotoxic anticancer drugs. *Ocul Surf*. 2021;21:221–237.
39. He J, Pham TL, Kakazu AH, Bazan HEP. Remodeling of Substance P sensory nerves and transient receptor potential melastatin 8 (TRPM8) cold receptors after corneal experimental surgery. *Invest Ophthalmol Vis Sci*. 2019;60:2449–2460.
40. Cho J, Bell N, Botzet G, et al. Latent sensitization in a mouse model of ocular neuropathic pain. *Transl Vis Sci Technol*. 2019;8:6.
41. Han Y, Smith MT. Pathobiology of cancer chemotherapy-induced peripheral neuropathy (CIPN). *Front Pharmacol*. 2013;4:156.
42. Yilmaz E, Gold MS. Sensory neuron subpopulation-specific dysregulation of intracellular calcium in a rat model of chemotherapy-induced peripheral neuropathy. *Neuroscience*. 2015;300:210–218.
43. Jin HW, Flatters SJ, Xiao WH, Mulhern HL, Bennett GJ. Prevention of paclitaxel-evoked painful peripheral neuropathy by acetyl-L-carnitine: effects on axonal mitochondria, sensory nerve fiber terminal arbors, and cutaneous Langerhans cells. *Exp Neurol*. 2008;210:229–237.
44. Hori J, Yamaguchi T, Keino H, Hamrah P, Maruyama K. Immune privilege in corneal transplantation. *Prog Retin Eye Res*. 2019;72:100758.
45. Gornstein EL, Schwarz TL. Neurotoxic mechanisms of paclitaxel are local to the distal axon and independent of transport defects. *Exp Neurol*. 2017;288:153–166.
46. Gornstein E, Schwarz TL. The paradox of paclitaxel neurotoxicity: mechanisms and unanswered questions. *Neuropharmacology*. 2014;76(pt A):175–183.
47. Pease-Raissi SE, Pazyra-Murphy MF, Li Y, et al. Paclitaxel reduces axonal Bclw to initiate IP3R1-dependent axon degeneration. *Neuron*. 2017;96:373–386.e376.
48. Ko MH, Hu ME, Hsieh YL, Lan CT, Tseng TJ. Peptidergic intraepidermal nerve fibers in the skin contribute to the neuropathic pain in paclitaxel-induced peripheral neuropathy. *Neuropeptides*. 2014;48:109–117.
49. Hara T, Chiba T, Abe K, et al. Effect of paclitaxel on transient receptor potential vanilloid 1 in rat dorsal root ganglion. *Pain*. 2013;154:882–889.
50. Li Y, North RY, Rhines LD, et al. DRG voltage-gated sodium channel 1.7 is upregulated in paclitaxel-induced neuropathy in rats and in humans with neuropathic pain. *J Neurosci*. 2018;38:1124–1136.
51. Zhou B, Wang DD, Qiu Y, et al. Boosting NAD level suppresses inflammatory activation of PBMCs in heart failure. *J Clin Invest*. 2020;130:6054–6063.
52. Elhassan YS, Kluckova K, Fletcher RS, et al. Nicotinamide riboside augments the aged human skeletal muscle NAD^+ metabolome and induces transcriptomic and anti-inflammatory signatures. *Cell Rep*. 2019;28:1717–1728.e1716.

Investigative Ophthalmology & Visual Science